
Active Peptides Derived from Snail Mucus Promoted Wound Healing by Enhancing Endothelial Cell Proliferation and Angiogenesis

[Guangqiang Li](#)[†], Yucheng Shi[†], Kehan Zhu, Bo Hu, Xianchen Huang, Yuan Sun, [Junmei Zhu](#)^{*}, [Duxin Li](#)^{*}, [Xicheng Zhang](#)^{*}

Posted Date: 24 June 2025

doi: 10.20944/preprints202506.1943.v1

Keywords: snail mucus; active peptides; endothelial cells; proliferation; wound healing



Preprints.org is a free multidisciplinary platform providing preprint service that is dedicated to making early versions of research outputs permanently available and citable. Preprints posted at Preprints.org appear in Web of Science, Crossref, Google Scholar, Scilit, Europe PMC.

Copyright: This open access article is published under a Creative Commons CC BY 4.0 license, which permit the free download, distribution, and reuse, provided that the author and preprint are cited in any reuse.

Disclaimer/Publisher's Note: The statements, opinions, and data contained in all publications are solely those of the individual author(s) and contributor(s) and not of MDPI and/or the editor(s). MDPI and/or the editor(s) disclaim responsibility for any injury to people or property resulting from any ideas, methods, instructions, or products referred to in the content.

Article

Active Peptides Derived from Snail Mucus Promoted Wound Healing by Enhancing Endothelial Cell Proliferation and Angiogenesis

Guanqiang Li ^{1,†}, Yucheng Shi ^{1,†}, Kehan Zhu ², Bo Hu, Xianchen Huang, Yuan Sun, Junmei Zhu ^{1,*}, Duxin Li ^{2,*} and Xicheng Zhang ^{1,*}

¹ Department of Vascular Surgery, The Medical Center of Soochow University, The Medical Center of Soochow University, Suzhou 215000, China

² College of Pharmaceutical Sciences, Soochow University, Suzhou 215021, China

* Correspondence: Correspondence: 13405093661@163.com (J.Z.); duxin.li@suda.edu.cn (D.L.); vasdoc@126.com (X.Z.)

[†] These authors equally contributed to this work.

Abstract

Snail mucus is significant in promoting wound healing, however, its active components and their mechanisms are partially understood. The present study isolated and hydrolyzed snail mucus via trypsin to obtain snail mucus active peptides (SMAP). The SMAP was analyzed via liquid chromatography mass spectrometry and bioinformatics screening, an active peptide EK-12 (molecular weight, 1366.2 Da) comprising 12 amino acids was screened from the candidate peptides and synthesized through the solid-phase approach. In vitro functional verification showed that EK-12 significantly promoted the proliferation, migration, and tube formation ability of endothelial cells. In vivo experiment showed that EK-12 significantly accelerated the wound healing process on mice. Pathological examinations showed significantly upregulated expression of CD31 and vascular endothelial growth factor in wound tissues, suggesting this as the mechanism by which the active peptide promoted angiogenesis and wound healing. Thus, the active peptide screened from snail mucus showed a great potential in developing therapeutic agent for wound healing.

Keywords: snail mucus; active peptides; endothelial cells; proliferation; wound healing

1. Introduction

Skin is the largest organ of human body, which prevents from external injury and infections[1]. Skin injury is often caused by trauma, surgery, infection, and diseases, such as diabetes. The natural healing process of skin injury is relatively slow and wound infection is often prone to occur. Thus, the discovery of bioactive components and explore its therapeutic mechanism is a hot topic of academic research[2].

Skin injury repair and regeneration is a complex process, consisted of mainly four stages, including hemostasis, inflammation, proliferation, and remodeling[3]. The activation of various cells such as endothelial cells (ECs), fibroblasts, and macrophages, as well as the synchronous interaction of cytokines and growth factors, are involved[4]. Angiogenesis is crucial in wound healing, as local injury-induced hypoxia and inflammatory factors stimulate EC proliferation and migration, gradually forming new epithelium, blood vessels, and granulation tissue. The newly formed capillary network provides oxygen, nutrients, and immune cells to the damaged tissue while facilitating the removal of metabolic waste, promoting wound healing[5-8].

Snail mucus has a long history of application in wound management. Current evidence suggests that snail mucus enhances fibroblast proliferation and migration, likely through the induction of interleukin-8 (IL-8) and other unidentified growth factors, thereby directly or indirectly accelerating

wound closure[9]. Furthermore, snail mucus-treated wounds demonstrate upregulated expression of angiogenic genes and enhanced matrix deposition, indicating its regulatory role in angiogenesis[10].

Our previous review on its chemicals found that snail mucus contains abundant natural collagen, allantoin, proteins, and glycosaminoglycans[11]. Recent studies reported that the mucin and polysaccharides promoted the wound healing process via functioning as adhesive agent[12,13]. Dolashki et al reported various peptides identified from snail mucus showing antimicrobial activities[14]. Despite these advances, the specific bioactive components and molecular mechanisms underlying snail mucus's therapeutic effects remain poorly understood. Therefore, the present study aimed to screen snail mucus active peptides (SMAPs) for wound healing and explore its potential mechanism. The results will provide the basis the development of natural drugs to promote wound healing in the future.

2. Materials and Methods

2.1. Preparation of Snail Mucus Lyophilized Powder

Fresh adult *Achatina fulica* snails with a body mass of over 20 g each were provided by Qianfu Company (Jiaxing, China), repeatedly rinsed with tap and distilled water, and placed in a rotating drum to stimulate mucus secretion. The collected mucus was dissolved in ultrapure water, centrifuged at $5,000 \times g$ for 10 min, and filtered through a $0.45\text{-}\mu\text{m}$ aqueous membrane to remove impurities. The supernatant was centrifuged at $3,000 \times g$ for 10 min, lyophilized, and stored as a lyophilized powder.

2.2. Enzymatic Hydrolysis of Snail Mucus

Lyophilized snail mucus powder (300 mg) was dissolved in 30 mL of 0.2 M disodium hydrogen phosphate-0.1 M citrate buffer (pH=6.8). Trypsin (6 mg, 2,500 U/mg activity) was added, and the mixture was incubated in a water bath at $37\text{ }^{\circ}\text{C}$ for 4 h. Subsequently, 10 mL of the reaction solution was heated at $100\text{ }^{\circ}\text{C}$ for enzyme inactivation and centrifuged at $5,000 \times g$ for 10 min. The supernatant was collected and then lyophilized to obtain a mixture containing snail mucus active peptides SMAP.

2.3. Screening and Synthesis of SMAP

The protein mixture of enzymatically hydrolyzed snail mucus was subjected to a standardized process of liquid chromatograph-mass spectrometry (Bruker timsTOF, USA) for proteomics studies and bioinformatics analysis. Then, Kyoto Encyclopedia of Genes and Genomes (KEGG) pathway enrichment analysis was used to annotate the function of the identified peptides. Peptides involved in the "Cell Growth and Death" regulatory pathway were selected and synthesized by Temic Biotech (Suzhou, China). The peptide was purified by high performance liquid chromatography (HPLC) and verified by mass spectrometry for molecular weight consistency (molecular weight error $<0.1\text{ Da}$). Peptides were stored as lyophilized powder and stored at $-20\text{ }^{\circ}\text{C}$, named as EK-12.

2.4. Cell Culture and Proliferation Assay

Human umbilical vein endothelial cells (HUVECs, Zhong Sheng, Beijing, China) were thawed and cultured in an endothelial cell medium (ECM) supplemented with 10% fetal bovine serum (FBS). Cells were passaged at 80–90% confluence and maintained for subsequent experiments. EK-12 were dissolved in sterile phosphate-buffered saline (PBS) to prepare drug solutions at concentrations of 10–3,000 $\mu\text{g/mL}$, using low (10–250 $\mu\text{g/mL}$) to high (500–3000 $\mu\text{g/mL}$) dose ranges to assess dose-dependent effects.

HUVECs were seeded into 96-well plates (100 $\mu\text{L/well}$) and pre-cultured for 24 h in a $37\text{ }^{\circ}\text{C}$, 5% CO_2 incubator to ensure adhesion. Subsequently, the cells were then treated with SMAPs at varying concentrations or with a drug-free medium (control) for 24 h, with six replicates per group. After

treatment, 10 μL of cell counting kit-8 (CCK-8) reagent was added to each well, followed by a 2-h incubation. Absorbance at 450 nm was measured using a microplate reader to calculate cell viability.

2.5. Cell Scratch Test

HUVECs were seeded into 12-well plates at 2×10^5 cells/well and cultured to 100% confluence. A sterile 200 μL pipette tip was used to create uniform scratches on the monolayer. After washing with PBS to remove detached cells and debris, experimental wells were treated with SMAPs at designated concentrations (1,000, 1,500, and 2,000 $\mu\text{g}/\text{mL}$), while were treated with a standard medium. Cell migration was monitored at 6, 12, and 24 h post-scratch using an inverted phase-contrast microscope. The cell migration rate was calculated as follows:

$$CM(\%) = \frac{S_0 - S}{S_0} \times 100\%$$

CM = cell migration rate; S_0 = initial scratch area; S = remaining scratch area at observation time.

2.6. Tube Formation Assay

Matrigel was thawed at 4 $^{\circ}\text{C}$, diluted, and aliquoted (50 $\mu\text{L}/\text{well}$) into pre-chilled plates, avoiding bubble formation. The plates were incubated for 30–45 min at 37 $^{\circ}\text{C}$ to allow polymerization. HUVECs were trypsinized, resuspended in a medium containing SMAPs (1,500 $\mu\text{g}/\text{mL}$ final concentration), and seeded onto the Matrigel-coated wells. The control groups were treated with a drug-free medium. Cells were cultured in a 37 $^{\circ}\text{C}$, 5% CO_2 incubator, and tubular structures were imaged at 6, 12, and 24 h via microscopy. Tube network nodes were quantified using ImageJ software.

2.7. Pro-Wound Healing Assay of SMAPs

Healthy adult Kunming male mice (aged 7 weeks and weighing 30–45g) were obtained from Gema Gene Company (Suzhou, China, catered by license SYXK2024-0013). This study was approved by the Ethics Committee of the Medical Center of Soochow University (approval no.2021-210044), and conducted per ARRIVE guidelines.

The mice were accommodated for 1 week, anesthetized, and subjected to dorsal hair removal using electric clippers and depilatory cream. The skin was disinfected with 75% ethanol, eighteen full-thickness circular wounds (1 cm diameter) were established on the dorsum in six mice, which were randomly divided into the experimental and control groups and treated daily with 1,500 $\mu\text{g}/\text{mL}$ SMAP or saline, respectively. The SMAP was fabricated a vaseline paste at 1,500 $\mu\text{g}/\text{mL}$ and topically applied to mice where the control group was treated with vaseline. Wound areas were photographed on Days 0, 3, 7, 10 and 14 and quantified using ImageJ software, and the healing rate was calculated as follows:

$$HR(\%) = \frac{S_0 - S}{S_0} \times 100\%$$

HR=healing rate; S_0 = initial wound area; S = remaining wound area at observation time.

2.8. Histopathological Examination

Post-euthanasia, wound tissues were excised, rinsed in saline, and fixed in paraffin. The sections were stained with hematoxylin and eosin (HE) for histological evaluation. Immunofluorescence staining for CD31 (endothelial marker) and vascular endothelial growth factor (VEGF) was performed to assess microvascular density and angiogenesis.

2.9. Statistical Analysis

Data were analyzed via SPSS 27.0. Continuous variables were presented as mean \pm standard deviation (SD) (normal distribution) or median (interquartile range, IQR) (non-normal distribution). Categorical variables are expressed as frequency (percentage) (n%). Group comparisons utilized

independent samples t-test (continuous data) or Chi-Square test (categorical data). Graphs were generated using Origin 2024, with error bars denoting SD or SEM. Statistical significance was denoted as: (* $P < 0.05$, ** $P < 0.01$, *** $P < 0.001$).

3. Results

3.1. Screening and Synthesis of SMAPs

The proteins were isolated from snail mucus and subjected to trypsin digestion to SMAPs. Through a standardized proteomics study process, 621 candidate peptides were identified from SMAPs and they were functionally annotated, as shown in Figure. 1A. Eighty-eight peptides were identified to be involved in basic Cellular Processes, and 12 peptides were further screened to be directly involved in the regulation of "Cell Growth and Death" pathways. Because small-molecular peptides are readily transported across the membrane and have relatively high bioavailability, a molecular weight threshold of $< 3,000$ Da was set as the screening threshold. From the 12 target peptides, EK-12 (N-terminal sequence: EAFDDAISELEK, Figure. 1B) with a molecular weight of 1366.2Da was selected. It was synthesized by solid-phase peptides synthesis method and purified by HPLC (C18 column, acetonitrile/water gradient elution), and the purity was $\geq 98\%$. The sequence of synthesized EK-12 was confirmed by MS/MS analysis (Figure 1).

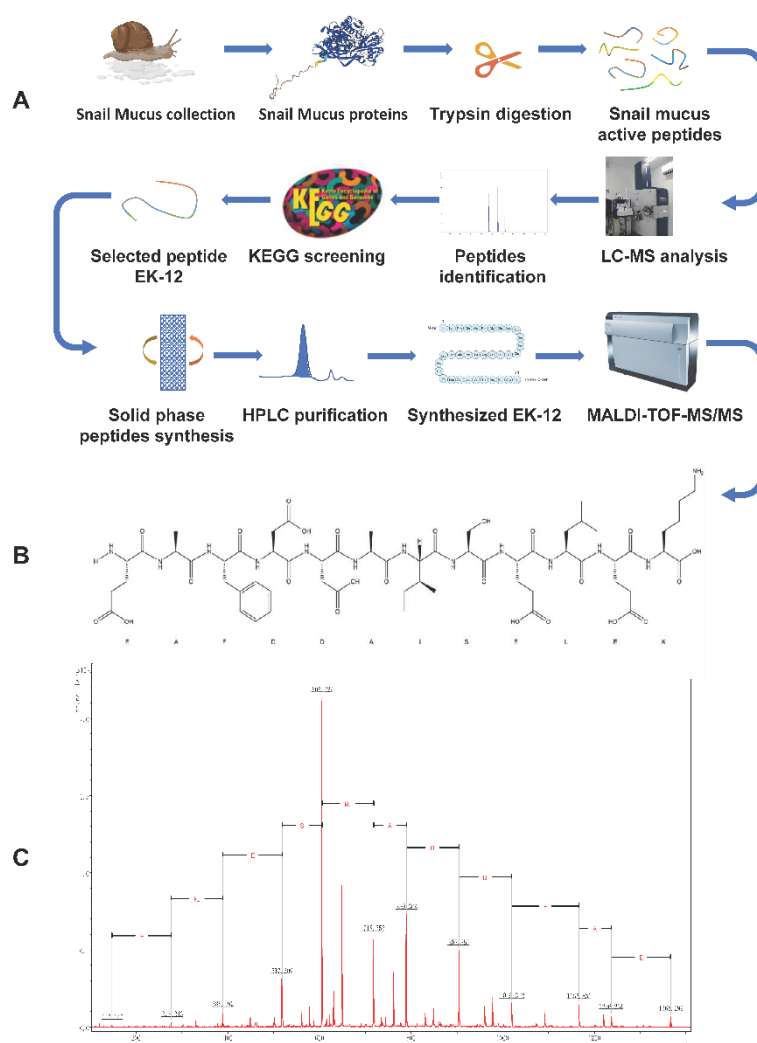


Figure 1. Screening and synthesis of SMAP (A). Research procedure of screening and synthesis of SMAP; (B). Synthetic EK-12 amino acid sequence; (C) MS/MS spectrum of synthesized EK-12.

3.2. Effects of EK-12 on Cell Proliferation

Compared with that in the control group, the CCK-8 assay (absorbance at 450 nm) showed that the proliferative activity of HUVECs under each SMAP in the experimental group was significantly increased, and the difference was statistically significant ($P < 0.01$). This proliferative effect was concentration-dependent and significantly increased with increasing EK12 concentration ($P < 0.01$). Notably, at 1,500 $\mu\text{g/mL}$ EK-12, the proliferative ability stopped increasing with the concentration, and there was no statistically significant difference between 1,500 and 3,000 $\mu\text{g/mL}$ ($P > 0.05$), indicating that the proliferative effect plateaued at 1,500 $\mu\text{g/mL}$ (Figure 2).

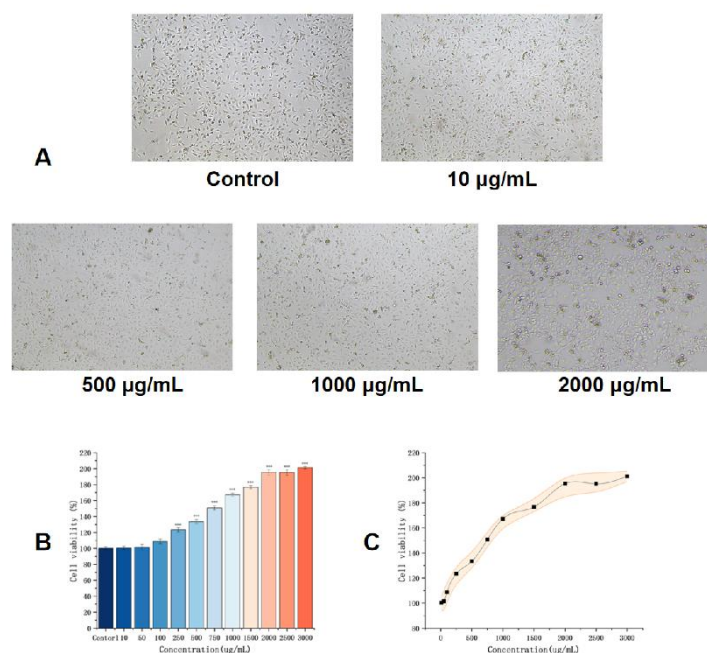


Figure 2. EK12 promotes HUVEC proliferation in a concentration-dependent manner (A) . Phase-contrast images illustrating HUVECs morphology. (B). Quantitative analysis cell proliferative activity across all tested concentrations compared to the control group ($P < 0.001$). (C) Effect on cell proliferation was enhanced with increasing concentration.

3.3. Effects of EK12 on Cell Migration

Based on CCK-8 results, EK12 at 1,000, 1,500, and 2,000 $\mu\text{g/mL}$ were selected for cell scratch assays. All concentrations significantly increased HUVECs migration rates compared that in the control group at 6, 12, and 24 h post-scratch ($P < 0.001$), with concentrations greater than 1,500 $\mu\text{g/mL}$ exerting a more significant effect; however, the 1,500 and 2,000 $\mu\text{g/mL}$ groups showed no significant differences ($P > 0.05$) (Figure 3).

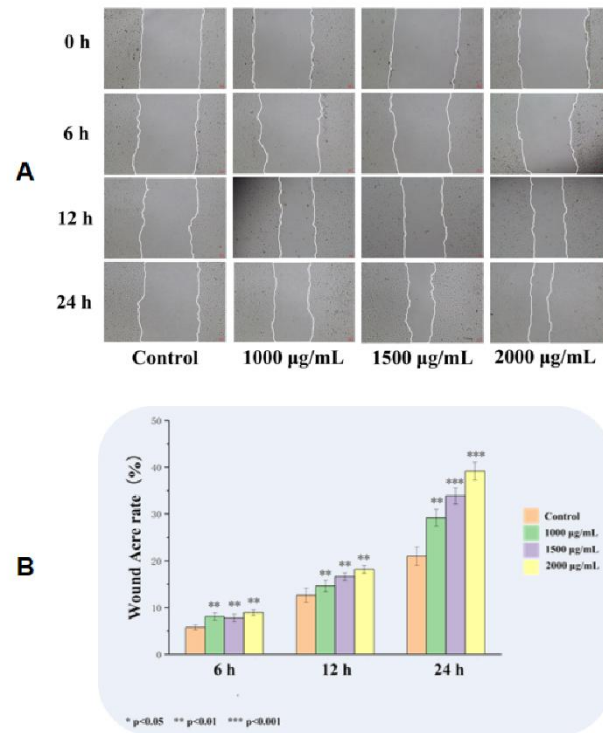


Figure 3. EK12 promote HUVECs migration. (A) Representative phase-contrast images of scratch wounds at 0-24 h post-treatment; (B). Effect at EK12 at 1,000, 1,500, and 2,000 µg/mL significantly increased HUVECs migration rates compared to the control group ($P < 0.001$).

3.4. Effects on Tube Formation Capacity

Compared with the observation in saline control group, EK12 at 1,000, 1,500 and 2,000 µg/mL significantly increased the number of HUVECs forming tubular structures on Matrigel after 24 h in a concentration-dependent manner. However, there was no significant difference between the 1,500 µg/mL and 2,000 µg/mL concentration groups ($P > 0.05$)(Figure.4).

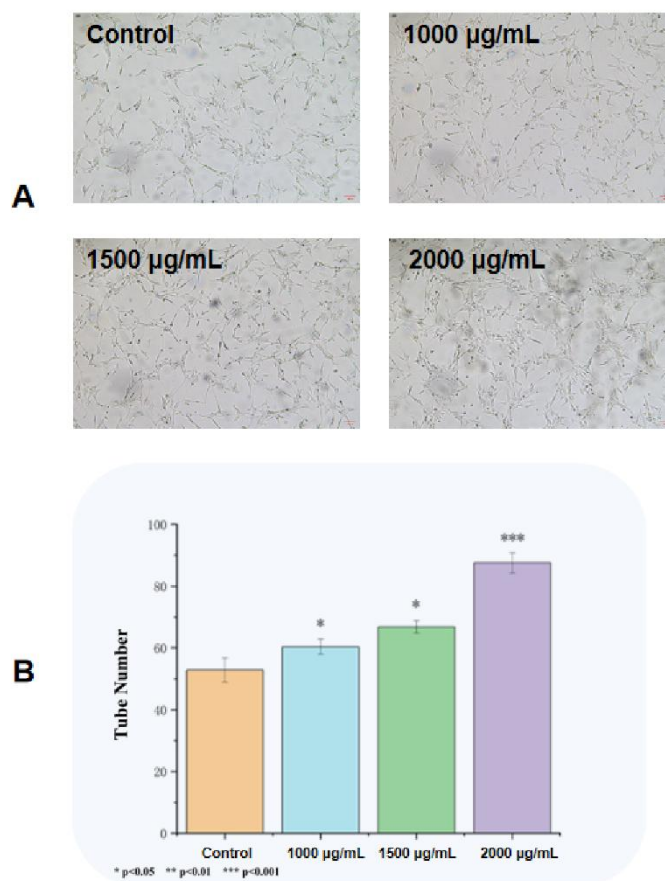


Figure 4. EK12 promotes tube formation capacity (24-h treatment). (A) Microscopic images of tubular network formation by HUVECs treated with varying EK12 concentrations. (B) .Tube formation ability at different concentrations.

3.5. Effects on Wound Healing and Angiogenesis

The wounds in the EK12 groups healed completely within 14 days, and the healing speed was significantly faster than that in the control group (Figure 5A-C). On day 7, the HR in the EK12 groups was significantly higher than that in the control group ($P < 0.01$). Immunofluorescence analysis further revealed elevated expression of CD31 (endothelial marker) and VEGF (angiogenic factor) in SMAP-treated tissues, as evidenced by higher mean fluorescence intensity ($P < 0.05$ and $P < 0.01$, respectively; Figure 6).

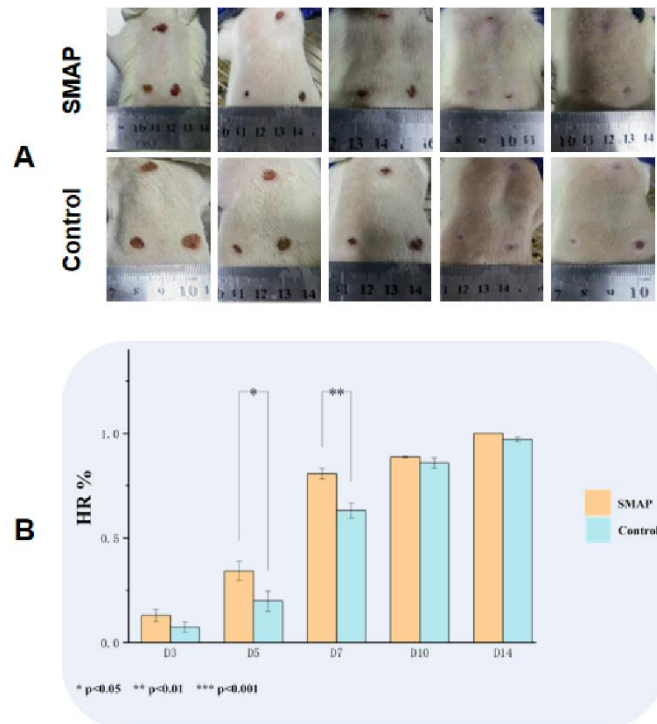


Figure 5. SMAPs accelerate wound healing in a mouse model. (A) Macroscopic images of wound healing progression in EK12-treated and control groups. (B). Time course analysis showed that the HR in the EK12 groups were significantly higher than that in the control group ($P < 0.05$, $P < 0.01$, $P < 0.001$). (C). Comparative wound healing profiles at key time points (Days 3, 7, 10, and 14).

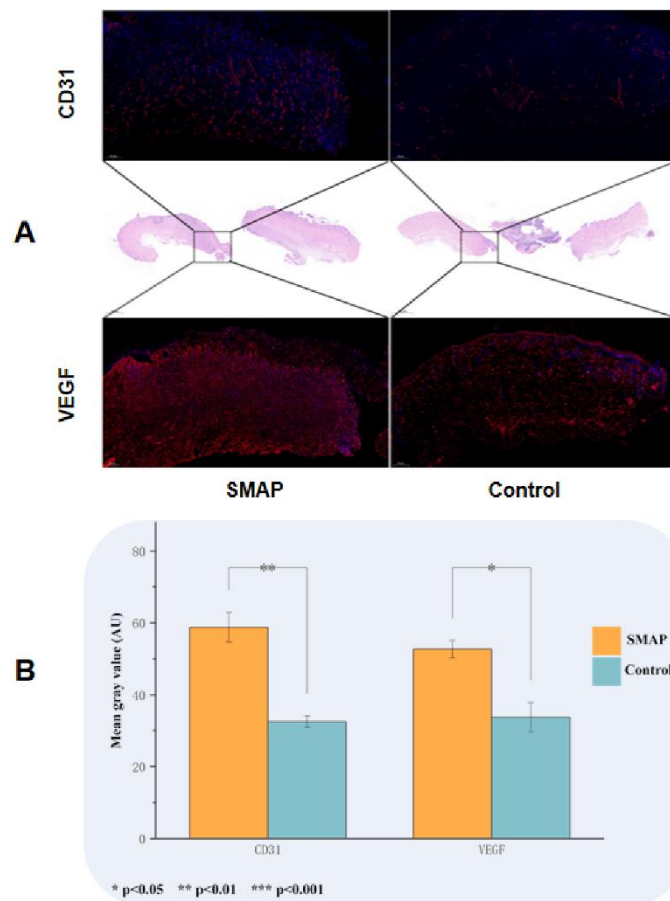


Figure 6. SMAPs upregulates angiogenic markers in wound tissues. (A). Immunofluorescence staining of CD31 and VEGF in EK12-treated and control tissues. EK12-treated samples exhibited markedly stronger fluorescence signals for both markers. (B) Semi-quantitative analysis of CD31 and VEGF expression (mean gray values) confirmed significant upregulation in the EK12 group ($P < 0.05$, $P < 0.01$).

4. Discussion

In chronic wounds, such as diabetic foot ulcers, persistent inflammation, microcirculatory dysfunction, and impaired ECs activity collectively suppress angiogenesis and extracellular matrix remodeling, significantly hindering healing[14]. Thus, protecting ECs from apoptosis and promoting localized vascularization are pivotal strategies in wound management[15]. Therefore, the present study used ECs for evaluating the effect of SMAP promoting wound healing.

Snail mucus has abundant active peptides that promote cell proliferation and antibacterial effects[11,16]. In this study, an active peptide derived from snail mucus was screened and synthesized for the first time, which significantly enhanced the proliferation, migration and tube formation of ECs. In vivo, EK-12 treatment upregulated VEGF and CD31 expression, facilitating collagen deposition and capillary network formation, which improved local blood perfusion and accelerated wound healing[17].

Mechanistically, we hypothesized that EK-12 (EAFDDAISELEK) may activate cell surface receptors (e.g., VEGFR-2) through the synergistic action of multiple targets and trigger downstream signaling pathways such as PI3K/AKT and MAPK/ERK. These pathways regulate cell cycle progression, survival, and angiogenesis, ultimately contributing to functional vascular network formation[18-20]. These findings highlight SMAP's potential as a therapeutic agent for ischemic ulcers. Furthermore, this study revealed that the ability of EK-12 to promote cell proliferation is concentration-dependent. Cellular proliferative and migratory activities increased with increasing EK-12 concentration. However, beyond a certain saturation concentration, cellular activity entered a plateau phase. This indicates that at this concentration, EK-12 may trigger a negative feedback mechanism regulating cell proliferation and/or reach a state of receptor binding saturation, leading to the cessation of increasing proliferative activity with additional concentration increases.

It is speculated that the snail mucus also contains various unidentified active peptide components and synergistic factors, which collaborate to promote wound healing[13]. Future studies should focus on isolating and synthesizing other individual peptides, characterizing their biological functions, and elucidating their molecular mechanisms. These efforts may provide new insights into ischemic vascular disease treatment and regenerative medicine.

5. Conclusion

The present study has screened a snail mucus derived peptide, EK-12. The EK-12 was synthesized and its sequence was confirmed via MS/MS analysis which is EAFDDAISELEK. EK-12 significantly promoted endothelial cell proliferation, migration, angiogenesis, and capillary network formation. EK-12 treatment had accelerated wound healing process on mice. The mechanism of EK-12 promoted wound healing was probably through multiple signaling pathways. These findings provide a scientific foundation for developing snail mucus-based therapeutics and offer a new approach to managing chronic wounds.

Author Contributions: Conceptualization, Zhang.X, Li.D and Zhu.J; methodology, Li.G and ZHu.K; software, Shi.Y, and H.B; validation, Z.X, and L.D.; formal analysis, H.X. and S.Y.; investigation, L.G.; resources, L.G. and Z.K.; data curation, L.G. and S.Y.; writing—original draft preparation, L.G.; writing- review and editing, L.G. and Z.J.; visualization, H.X.; supervision, L.D.; project administration, Z.X. and L.D.; funding acquisition, Z.X. All authors have read and agreed to the published version of the manuscript.

Funding: This work was financially supported by the Suzhou Science and Technology Bureau's Science and Technology Program Fund (SZM2021008), and supported by the Gusu Talent Program of Suzhou Health Commission (GSWS2022118), and Healthcare Innovation Research Program (CXYJ2024B08).

Institutional Review Board Statement: This study was approved by the institutional ethics review committee of the Medical Center of Soochow University (approval code: 2021-210044; approval date: 19 August 2021).

Data Availability Statement: Not applicable.

Conflicts of Interest: The authors declare no conflict of interest.

Reference

1. Xu, C.; Wang, F.; Guan, S.; Wang, L. β -Glucans obtained from fungus for wound healing: A review. *Carbohydr. Polym.* 2024, 327, 121662. DOI: <https://doi.org/10.1016/j.carbpol.2023.121662>.
2. Zhu, K.; Yao, Z.; Gu, T.; Jiang, X.; Zhou, J.; Li, D. Study of the ability of polysaccharides isolated from *Zizania latifolia* to promote wound healing in mice via in vitro screening and in vivo evaluation. *Food Chem* 2025, 464 (Pt 3), 141810. DOI: 10.1016/j.foodchem.2024.141810 From NLM Medline.
3. Nourian Dehkordi, A.; Mirahmadi Babaheydari, F.; Chehelgerdi, M.; Raeisi Dehkordi, S. Skin tissue engineering: Wound healing based on stem-cell-based therapeutic strategies. *Stem Cell Res Ther* 2019, 10, 111. DOI:10.1186/s13287-019-1212-2.
4. Toshikazu, K.; Yuko, I. Molecular pathology of wound healing. *Forensic Sci Int* 2010, 15, 93–98.
5. Huang, C.; Teng, J.; Liu, W.; Wang, J.; Liu, A. Modulation of macrophages by a phyllyrin-loaded thermosensitive hydrogel promotes skin wound healing in mice. *Cytokine* 2024, 177, 156556. DOI:10.1016/j.cyto.2024.156556.
6. Kim, H.S.; Sun, X.; Lee, J.H.; Kim, H.W.; Fu, X.; Leong, K.W. Advanced drug delivery systems and artificial skin grafts for skin wound healing. *Adv Drug Deliv Rev* 2019, 146, 209–239. DOI:10.1016/j.addr.2018.12.014.
7. Sorg, H.; Sorg, C.G.G. Skin wound healing: Of players, patterns, and processes. *Eur Surg Res* 2023, 64, 141–157. DOI:10.1159/000528271.
8. Werner, S.; Grose, R. Regulation of wound healing by growth factors and cytokines. *Physiol Rev* 2003, 83, 835–870. DOI:10.1152/physrev.2003.83.3.835.
9. Ricci, A.; Gallorini, M.; Feghali, N.; Sampò, S.; Cataldi, A.; Zara, S. Snail slime extracted by a cruelty free method preserves viability and controls inflammation occurrence: A focus on fibroblasts. *Molecules* 2023, 28, 1222. DOI:10.3390/molecules28031222.
10. Sun, L.; Wang, X.; Deng, T.; Luo, L.; Lin, L.; Yang, L.; Tian, Y.; Tian, Y.; Wu, M. Bionic sulfated glycosaminoglycan-based hydrogel inspired by snail mucus promotes diabetic chronic wound healing via regulating macrophage polarization. *Int J Biol Macromol* 2024, 281, 135708. DOI:10.1016/j.ijbiomac.2024.135708.
11. Zhu, K.; Zhang, Z.; Li, G.; Sun, J.; Gu, T.; Ain, N.U.; Zhang, X.; Li, D. Extraction, structure, pharmacological activities and applications of polysaccharides and proteins isolated from snail mucus. *Int J Biol Macromol* 2024, 258, 128878. DOI:10.1016/j.ijbiomac.2023.128878.
12. McDermott, M.; Cerullo, A. R.; Parziale, J.; Achrak, E.; Sultana, S.; Ferd, J.; Samad, S.; Deng, W.; Braunschweig, A. B.; Holford, M. Advancing Discovery of Snail Mucins Function and Application. *Front. Bioeng. Biotechnol.* 2021, Volume 9 - 2021, Mini Review. DOI: 10.3389/fbioe.2021.734023.
13. Deng, T.; Gao, D.; Song, X.; Zhou, Z.; Zhou, L.; Tao, M.; Jiang, Z.; Yang, L.; Luo, L.; Zhou, A.; et al. A natural biological adhesive from snail mucus for wound repair. *Nat Commun* 2023, 14 (1), 396. DOI: 10.1038/s41467-023-35907-4.
14. Dolashki, A.; Velkova, L.; Daskalova, E.; Zheleva, N.; Topalova, Y.; Atanasov, V.; Voelter, W.; Dolashka, P. Antimicrobial Activities of Different Fractions from Mucus of the Garden Snail *Cornu aspersum*. *Biomedicines* 2020, 8 (9). DOI: 10.3390/biomedicines8090315.
15. Dasari, N.; Jiang, A.; Skochdopole, A.; Chung, J.; Reece, E.M.; Vorstenbosch, J.; Winocour, S. Updates in diabetic wound healing, inflammation, and scarring. *Semin Plast Surg* 2021, 35, 153–158. DOI:10.1055/s-0041-1731460.

16. Huang, L.; Cai, H.A.; Zhang, M.S.; Liao, R.Y.; Huang, X.; Hu, F.D. Ginsenoside Rg1 promoted the wound healing in diabetic foot ulcers via miR-489-3p/Sirt1 axis. *J Pharmacol Sci* **2021**, *147*, 271–283. DOI:10.1016/j.jphs.2021.07.008.
 17. You, Y.; Tian, Y.; Guo, R.; Shi, J.; Kwak, K.J.; Tong, Y.; Estania, A.P.; Hsu, W.H.; Liu, Y.; Hu, S.; et al. Extracellular vesicle-mediated VEGF-A mRNA delivery rescues ischaemic injury with low immunogenicity. *Eur Heart J* **2025**, *46*, 1662–1676. DOI:10.1093/eurheartj/ehae883.
 18. Wu, M.; Huang, J.; Shi, J.; Shi, L.; Zeng, Q.; Wang, H. Ruyi Jinhuang Powder accelerated diabetic ulcer wound healing by regulating Wnt/ β -catenin signaling pathway of fibroblasts in vivo and in vitro. *J Ethnopharmacol* **2022**, *293* (Suppl c), 115321. DOI:10.1016/j.jep.2022.115321.
 19. Mo, J.; Zhang, J.; Meng, X.; Wang, F.; Tang, W.; Liu, Y.; Fu, L.; Liang, F.; Mo, Z. Inhibition of microRNA-139-5p improves fibroblasts viability and enhances wound repair in diabetic rats through AP-1 (c-Fos/c-Jun). *Diabetes Metab Syndr Obes* **2025**, *18*, 237–248. DOI:10.2147/DMSO.S496556.
- Zhu, J.; Zhang, M.; Gao, Y.; Qin, X.; Zhang, T.; Cui, W.; Mao, C.; Xiao, D.; Lin, Y. Tetrahedral framework nucleic acids promote scarless healing of cutaneous wounds via the AKT-signaling pathway. *Signal Transduct Target Ther* **2020**, *5*, 120. DOI:10.1038/s41392-020-0173-3.

Disclaimer/Publisher's Note: The statements, opinions and data contained in all publications are solely those of the individual author(s) and contributor(s) and not of MDPI and/or the editor(s). MDPI and/or the editor(s) disclaim responsibility for any injury to people or property resulting from any ideas, methods, instructions or products referred to in the content.